Deep Traps Distribution in $TlInS_2$ Layered Crystals

M. Isik[a,*], N.M. Gasanly[b] and H. Ozkan[b]

[a]Department of Electrical and Electronics Engineering, Atilim University
06836 Ankara, Turkey

[b]Department of Physics, Middle East Technical University
06531 Ankara, Turkey

(Received September 29, 2008; in final form November 24, 2008)

The trap centers and distributions in $TlInS_2$ were studied in the temperature range of 100–300 K by using thermally stimulated currents technique. Experimental evidence was found for the presence of three trapping centers with activation energies 400, 570, and 650 meV. Their capture cross-sections were determined as 6.3×10^{-16}, 2.7×10^{-12}, and 1.8×10^{-11} cm^2, respectively. It was concluded that in these centers retrapping is negligible as confirmed by the good agreement between the experimental results and the theoretical predictions of the model that assumes slow retrapping. An exponential distribution of hole traps was revealed from the analysis of the thermally stimulated current data obtained at different light excitation temperatures. This experimental technique provided a value of 800 meV/decade for the trap distribution.

PACS numbers: 71.55.−i, 72.20.Jv, 72.80.Jc

1. Introduction

$TlInS_2$ belongs to the III–III–VI_2 family of crystals known as thallium dichalcogenides. Members of this family have both layered ($TlGaS_2$, $TlGaSe_2$, $TlInS_2$) and chain ($TlInSe_2$, $TlInTe_2$, $TlGaTe_2$) structures. They have become interesting due to their interesting structural properties and potential optoelectronic applications [1]. Their quasi-low dimensionality, optical and photoconductive properties and other features attract the attention of researchers to study these compounds. At room temperature, the layered crystal $TlInS_2$ belongs to the monoclinic system with a space group $C2/c$ and consists of a 1:1 ratio of InS:TlS. The crystal lattice has two-dimensional layers arranged parallel to the (001) plane. Each successive layer is turned through a right angle to the preceding one.

$TlInS_2$ is pretty useful crystal for optoelectronic applications thanks to its high photosensitivity in the visible range of spectra and high birefringence in conjunction with a wide transparency range of 0.5–14 μm [2, 3]. For possible applications as an optoelectronic device in the visible range, a great deal of attention has been devoted to the study of the structural [1, 4–7], electrical [8–10], and optical [8, 11–14] properties. These properties of semiconductors differ due to individual characteristics of energy gaps and impurities. The determination of activation energies of trapping centers in the energy gap takes an important role in the study of the properties of semiconductors. It was determined that the forbidden energy gap of $TlInS_2$ was found to be a direct band gap with an energy of 2.58 eV at $T = 10$ K by measuring both absorption and reflection spectroscopy as a function of temperature [11, 12]. Optical properties of $TlInS_2$ were also studied in Refs. [8, 15, 16]. It was revealed that $TlInS_2$ crystals have two energy gaps, consisting of a direct and an indirect one, which were found to be equal to 2.28 and 2.23 eV at 300 K, respectively. Photoluminescence (PL) spectra of $TlInS_2$ and their temperature and excitation intensity dependences in the 500–860 nm wavelength region have been reported in Ref. [17]. In this study, two PL bands centered at 515 nm (2.41 eV, A-band) and 816 nm (1.52 eV, B-band) at $T = 11.5$ K and excitation intensity of 7.24 W/cm^2 were observed. Analysis of the experimental data revealed that emission A-band was due to radiative transitions from shallow donor level located at 20 meV below the bottom of the conduction band to the moderately deep acceptor level located at 250 meV above the top of the valence band.

One of the methods used to determine the properties of traps in semiconductors is thermally stimulated current (TSC) technique. TSC measurements have been extensively carried out in the past in the crystals which is very useful to fabricate high quality devices [18–22]. There are a few studies in the literature in which TSC technique is used to determine the trapping parameters in $TlInS_2$ single crystals. The shallow levels in the $TlInS_2$

* corresponding author; e-mail: misik@atilim.edu.tr

crystals in the temperature range below 90 K have been studied in Ref. [23]. In this study, the TSC measurements in $TlInS_2$ crystals over the temperature range of 10–90 K revealed that there was a trap level in the energy gap with activation energy of 12 meV. Özdemir et al. [24] have investigated the trap levels in $TlInS_2$ crystals by TSC spectroscopy in the temperature range of 90–200 K. Analysis of the experimental spectra represented a series of trap levels with energy depths ranging from 150 to 220 meV in the energy gap. Recently, we carried out TSC measurements on $TlInS_2$ layered crystals to study the shallow traps and their distribution in the temperature range of 10–100 K [25]. Two trapping centers, 12 and 14 meV, have been detected in this study. Also the experiments showed the presence of an exponential distribution of shallow trapping states in the crystal with a variation of one order of magnitude in the trap density for every 27 meV.

The purpose of the present work is to obtain detailed information concerning deep traps distribution in undoped $TlInS_2$ layered crystals in the temperature range 100–300 K by using TSC measurements. Besides, the TSC data were analyzed by using various methods. The activation energy, capture cross-section, attempt to escape frequency and concentration of traps for peaks observed in the TSC spectra of $TlInS_2$ crystals were determined.

2. Experimental details

$TlInS_2$ polycrystals were synthesized from high purity elements taken in stoichiometric proportions. Single crystals of $TlInS_2$ were grown by the Bridgman method without any intentional doping. The resulting ingots (orange in color) showed good optical quality and the freshly cleaved surfaces were mirror-like. The chemical composition of the crystals was determined by energy dispersive spectroscopic analysis using JSM-6400 electron microscope. The atomic composition ratio of the studied samples (Tl : In : S) was found to be 25.6 : 25.2 : 49.2, respectively. For TSC measurements a sample with dimensions of $6.0 \times 2.0 \times 1.5$ mm^3 were used. Electrical contacts were made on the sample surface with silver paste according to sandwich geometry. In the sandwich configuration, one of the electrodes is placed on the front surface of the crystal with a small droplet of silver paste. Then the sample is mounted on the sample holder with conducting silver paste. The second electrode is connected to the cryostat for circuit connection. The carriers flow through the crystal in the direction of parallel to the c-axis in the sandwich geometry. The electrical conductivity of the studied sample was n-type. The values of the room temperature electrical resistivity, carrier concentration, and Hall mobility were found to be 7.4×10^5 Ω cm, 3.0×10^{11} cm^{-3}, and 28 cm^2 V^{-1} s^{-1}, respectively.

The TSC measurements were performed in the temperature range from 100–300 K using an Advanced Research Systems closed-cycle helium cryostat. Constant heating rate was achieved by a Lake-Shore 331 temperature controller. A Keithley 228 A voltage/current source and a Keithley 6485 picoammeter were used for the TSC measurements. The temperature and current sensitivities of the system were about 10 mK and 2 pA, respectively. At low enough temperatures, when the probability of thermal release is negligible, a light emitting diode generating light at a maximum peak of 2.6 eV was used to excite the charge carriers. The trap filling was performed by illumination under bias voltage of $V_1 = 1$ V at the initial temperature $T_0 = 60$ K. When the illumination time is increased in a controlled way, it was observed that after nearly 20 min illumination, the traps are filled completely. Therefore, the illumination time was chosen as 20 min for TSC measurements. Then the excitation was turned off. After an expectation time ($\approx$ 300 s), the bias voltage of V_2 was applied to the sample and temperature was increased at constant rate. In $TlInS_2$ the dark current contribution was low, therefore the voltage of $V_2 = 100$ V can be applied during heating.

"Thermal cleaning" procedure was used to isolate the overlapping TSC peaks [21]. "Thermal cleaning" procedure was applied as follows: The sample was cooled and irradiated at 60 K. Then it was heated with the constant heating rate but stopped near the temperature of the first peak (T_{mA}). Traps responsible for the current peak for temperatures lower than the temperatures of the second (T_{mB}) and third (T_{mC}) peaks were substantially emptied by this way. Then, the crystal was recooled down to the initial temperature and reheated in the dark at the same heating rate. This allowed the observation of TSC peaks due to carriers released from the remaining filled traps.

TSC measurements can also be used to reveal the characteristic features of traps distribution. The experimental TSC procedure applied to study the traps distribution is as follows: the sample is excited by light at different excitation temperatures (T_0) to allow trapping of the photoproduced electrons. Then the light was turn off and the sample was recooled to initial temperature 60 K in darkness. Thereafter the sample was heated with a constant heating rate to excite the trapped electrons into the conduction band.

The carrier lifetime was determined from the photoconductivity decay experiments. In these experiments, two electrodes are attached to opposite surfaces of the $TlInS_2$ with silver paste. Then one of the contacts was illuminated by a high efficiency short-pulsed LED controlled by "NI USB-6211 high-performance USB data acquisition device". The signal was transmitted to the computer and then analyzed to determine the decay time of the photocurrent.

3. Results and discussion

3.1. Determination of the type of the charge carriers

Figure 1 shows a typical TSC curve of $TlInS_2$ crystal measured with heating rate of $\beta = 0.8$ K/s both for forward and reverse bias conditions in the 100–250 K

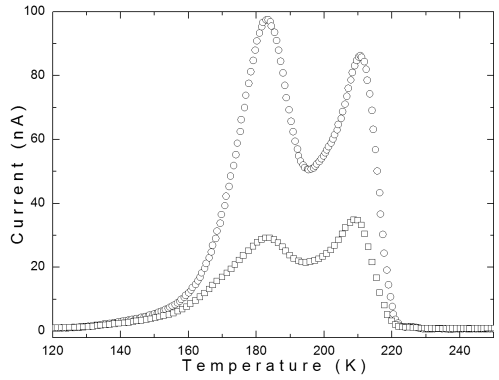

Fig. 1. Typical experimental TSC curves of $TlInS_2$ crystal under opposite bias voltage. Circles and squares represent the experimental data obtained at illumination of positive and negative contacts, respectively.

temperature range. When the sample is illuminated in proximity to a contact, both types of carriers are created near the contact. Then depending on the bias voltage, only one type of carrier will be swept through the entire field region, whereas the second type is collected very quickly. Therefore, only the former can be trapped. By illumination of the positive and negative contacts of the sample separately, the maximum TSC measured for the first peak equals 29 and 98 nA, respectively, and for the second peak equals 35 and 86 nA, respectively. The intensity of the current peak was highest when the polarity of the illuminated contact was positive. Therefore the trapping centers corresponding to these peaks can be characterized as hole traps.

3.2. Determination of activation energy

There are several methods to evaluate the trapping parameters from the experimental TSC spectra. Experimental TSC curves for $TlInS_2$ crystal have been analyzed by using curve fitting and initial rise methods.

3.2.1. Curve fitting method

The curve fitting method was used for decomposition of the TSC spectra into separate peaks associated with the charged traps in $TlInS_2$ crystal. Under monomolecular conditions (i.e., slow retrapping) the TSC curve of a discrete set of traps with a trapping level E_t is described by the equation [21]:

$$I = n_t \tau e \mu \nu (V_2/L) A \times \exp\left(-\frac{E_t}{kT} - \int_{T_0}^{T} \frac{\nu}{\beta} \exp\left(-\frac{E_t}{kT}\right) \mathrm{d}T\right). \quad (1)$$

Here, I is the thermally stimulated current, n_t is the initial density of filled traps, τ is the lifetime of a free carrier, e is the electronic charge, μ is the carrier mobility, ν is the attempt-to-escape frequency of a trapped carrier, V_2 is the applied voltage, A and L are the area and the length of the sample, respectively, k is the Boltzmann constant, β is the heating rate and T_0 is the temperature at which heating begins after filling the traps. If we assume ν to be independent of T and ignore the variation of μ and τ with T over the temperature span of the TSC curve, Eq. (1) can be rewritten as [26]:

$$I = A_0 \exp\left(-t - B \exp\left(-t\right) t^{-2}\right), \quad (2)$$

where $t = E_t/kT$, and A_0 and B are constants

$$A_0 = n_t \tau e \mu \nu (V_2/L) A \quad \text{and} \quad B = \frac{\nu E_t}{\beta k}. \quad (3)$$

If Eq. (2) is differentiated and equated with zero to find the maximum of the curve, which occurs at $t = t_m = E_t/kT_m$, then

$$B = \exp\left(t_m\right) \frac{t_m^3}{t_m + 2}. \quad (4)$$

In order to analyze the peaks simultaneously, the fitting function is given by the sum

$$I(T) = \sum_{i=1}^{n} I_i(T), \quad (5)$$

where $I_i(T)$ denotes the current contribution of each peak calculated by means of Eq. (2) and n denotes the number of traps involved in the calculation.

When the curve is fitted by means of three peaks (designated A, B and C), we obtained a good fit to the experimental data. The experimental data and theoretical curve, computed with the assumption of monomolecular conditions (slow retrapping) were completely agreed with each other (Fig. 2). This agreement suggests that retrapping does not occur for the observed traps. The solid line in Fig. 2 shows the data for a heating rate of 0.8 K/s fitted with three peaks (A, B and C) having activation energies of $E_{tA} = 400$ meV, $E_{tB} = 570$ meV and $E_{tC} = 650$ meV, respectively (Table I).

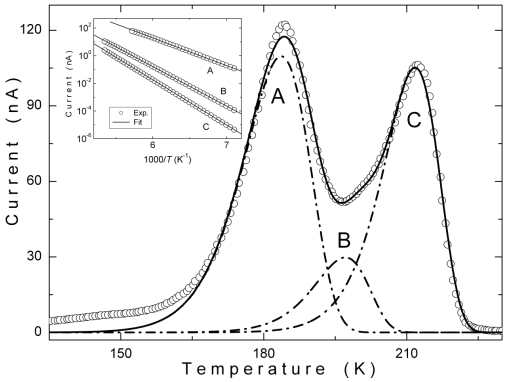

Fig. 2. Experimental TSC spectrum of $TlInS_2$ crystal with heating rate 0.8 K/s and decomposition of this spectrum into three separate peaks. Open circles are experimental data. Dash-dotted curves represent decomposed peaks. Solid curve shows total fit to the experimental data. Inset: thermally stimulated current vs. $1000/T$ for the A-, B- and C-peaks in the TSC spectrum of the $TlInS_2$ crystal. The circles show the experimental data, and the lines represent the theoretical fits obtained by using initial rise method.

TABLE I
Activation energy (E_t), capture cross-section (S_t), attempt-to-escape frequency (ν) and concentration (N_t) of traps for three TSC peaks of $TlInS_2$ crystal.

Peak	T_m [K]	E_t [meV] Curve fitting method	E_t [meV] Initial rise method	S_t [cm^2]	ν [s^{-1}]	N_t [cm^{-3}]
A	184	400	400	6.3×10^{-16}	9.6×10^{9}	4.1×10^{9}
B	197	570	570	2.7×10^{-12}	4.8×10^{13}	0.9×10^{9}
C	212	650	650	1.8×10^{-11}	3.7×10^{14}	2.6×10^{9}

"Thermal cleaning" procedure, described in the previous section, was used to isolate the overlapping A-, B- and C-peaks. The resultant thermally stimulated curve after thermal cleaning at temperature near T_{mA} is shown in Fig. 3. Due to low intensity of the B-peak, we could not observe this peak after thermal cleaning. Thus, the peak observed after thermal cleaning corresponds to the C-peak.

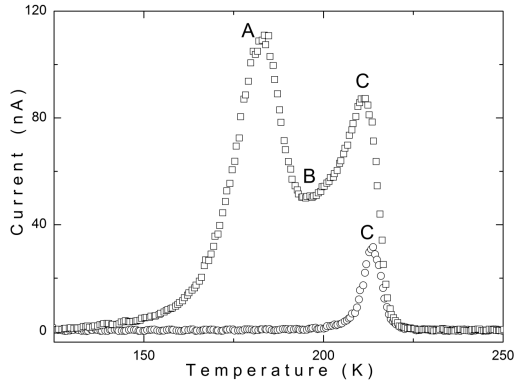

Fig. 3. Experimental TSC spectra of $TlInS_2$ crystal before (squares) and after (circles) thermal cleaning. Heating rate $\beta = 0.8$ K/s.

3.2.2. Initial rise method

The initial rise method, which is valid for all types of recombination kinetics, is based on the assumption that the TSC is proportional to $\exp(-E_t/kT)$ when the traps begin to empty with temperature [21]. Thus, a semi-logarithmic plot of the current versus $1/T$ gives a straight line with a slope of $(-E_t/k)$. The plots for TSC peaks of $TlInS_2$ crystal are shown in the inset of Fig. 2. The activation energies of the traps calculated by this method were found to be 400, 570 and 650 meV (Table I).

At this point, it is worthwhile to compare the results of present TSC analysis with those obtained by Özdemir et al. [24] on $TlInS_2$ crystals in the temperature range of 90–200 K. TSC spectra consisted of one pronounced ($T_m = 187$ K, $I_m = 65$ pA) and several non-distinct weak peaks at lower temperatures. As a result of decomposition of the spectra into separate peaks, the authors revealed six trap levels with activation energies of 150, 190, 200, 210, 212 and 220 meV and T_m = 102.0, 114.5, 124.5, 139.5, 153.0 and 187.0 K, respectively. The distinction in the number of the traps, activation energies and other parameters may be associated with difference in the single crystal growing conditions (thermal gradient, the rate of ampoule motion in two-zone furnace etc).

3.3. Determination of the traps distribution

Figure 4 shows the experimental TSC spectra (C-peak) for $TlInS_2$ crystal obtained at different excitation temperatures (T_0 = 105, 110, 115 and 120 K). The spectra decreased in intensity and shifted towards higher temperatures with increasing the light excitation temperature. This shift supports the validity of a quasi-continuous trap distribution [27–30].

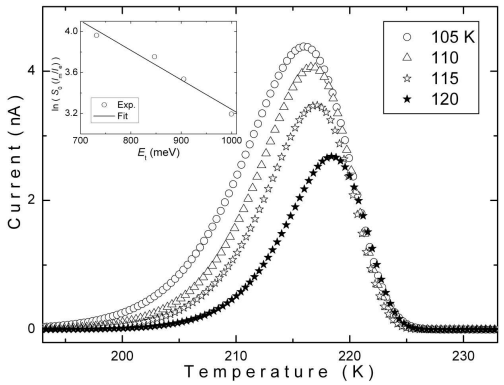

Fig. 4. Experimental TSC spectra (C-peak) of the $TlInS_2$ crystal at different excitation temperatures T_0. The heating rate was $\beta = 0.8$ K/s. Inset: $\ln(S_0(I_m/I_e))$ plot as a function of the activation energy E_t.

Each TSC spectra obtained at different excitation temperatures can be described by the following expression [27]:

$$I = C\nu \exp(-E_t/kT), \tag{6}$$

where C is a constant. $\ln(I)$ versus $1/T$ plots are the straight lines whose slopes give the values of activation energy E_t at each excitation temperature T_0. The activation energies obtained at different excitation temperatures and the maximum temperatures of thermocurrent curves were listed in Table II. The activation energy ranges from 730 to 1000 meV at T_0 = 105 and 120 K, respectively.

By assuming an exponential traps distribution, whose density at energy E_t will be given by $N = A_1 \exp(-\alpha E_t)$, we can write for the traps filled at the excitation temperature T_0 the following expression [27]:

$$S_0(I_m/I_e) \propto A_1 \exp(-\alpha E_t), \tag{7}$$

where α is the energy parameter which characterizes the distribution, I_m and I_e are the currents flowing in the crystal at the peak temperature in darkness and during light excitation, respectively, S_0 is the area of the TSC peak, which is proportional to the total number of

TABLE II

TSC parameters of C-peak for $TlInS_2$ crystal at different excitation temperatures.

Curve	1	2	3	4
excitation temperature [K]	105	110	115	120
maximum temperature [K]	216.0	216.7	217.1	218.0
curve area [arb. u.]	526	427	343	244
activation energy [meV]	730	850	905	1000

carriers released from the traps during the heating process. Inset of Fig. 4 shows the $\ln[S_0(I_m/I_e)]$ plotted as a function of the energy E_t, determined from the analysis of TSC curves, which were registered at different excitation temperatures. The graph obtained is a straight line with a slope $\alpha = 0.0029$ meV^{-1} corresponding to 800 meV/decade, an order of magnitude variation in the trap density for every 800 meV.

3.4. Determination of capture cross-section and concentration of the traps

After the values of E_t and T_m for peaks are determined by using curve fit method (Table I), the constant B and the attempt-to-escape frequency ν are calculated by using Eqs. (3) and (4). Then we can calculate the capture cross-section of the traps according to expression

$$S_t = \frac{\nu}{N_c v_{th}}, \tag{8}$$

where N_c is the effective density of states in the conduction band and v_{th} is thermal velocity of a free electron. For the calculation of N_c and v_{th} we used the electron effective mass $m_e^* = 0.14m_0$ reported for $TlInS_2$ crystals [10]. The results obtained for the capture cross-section and attempt-to-escape frequency of A-, B- and C-peaks are presented in Table I. Another indication which points out the assumption of monomolecular kinetics for the observed peaks is the small value of the capture cross-section.

The concentration of the traps was estimated using the relation

$$N_t = \frac{Q}{ALeG}. \tag{9}$$

Here, Q is the quantity of charge released during a TSC experiment and can be calculated from the area under the TSC peaks; e is the electronic charge and G is the photoconductivity gain, which equals to the number of carriers passing through the sample for each absorbed photon. The photoconductivity gain G was calculated from the expression [22]:

$$G = \frac{\tau}{t_{tr}} = \frac{\tau \mu V}{L^2}, \tag{10}$$

where τ is the carrier lifetime, t_{tr} is the carrier transit time between the electrodes and μ is the carrier mobility. To calculate the photoconductivity gain G, the carrier lifetime is obtained from the photoconductivity decay experiments. The photocurrent decay is nearly exponential after termination of light pulse at $t = t_0$. The carrier lifetime τ was determined from the corresponding output voltage expressed as [31]:

$$V_{ph} = V_{ph0} + D\exp(-t/\tau), \tag{11}$$

where V_{ph0} is the voltage at $t = \infty$ and D is a constant.

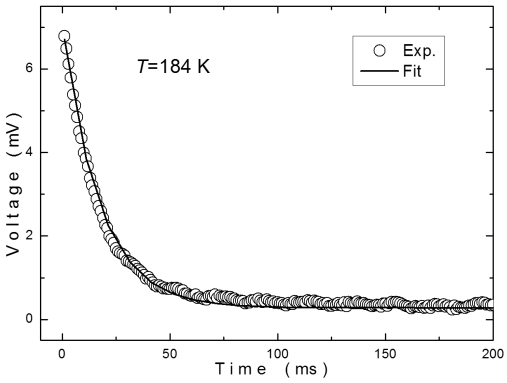

Fig. 5. Photoconductivity decay curve for the $TlInS_2$ crystal at $T = 184$ K. Open circles are experimental data. Solid line shows the fit to the experimental data.

Figure 5 shows the theoretical fit to the experimental data using Eq. (11) for $TlInS_2$ crystals at 184 K. The carrier lifetime was obtained as 17.2, 19.0 and 21.6 ms for temperatures 184, 197 and 212 K, respectively, from the decay of the photocurrent. The corresponding photoconductivity gain was calculated from Eq. (10) and found to be 2140, 2360 and 2690 using $V = 100$ V and $\mu = 28$ cm^2/(V s) [10]. Then the values of N_t obtained for traps are evaluated as 4.1×10^9 cm^{-3}, 0.9×10^9 cm^{-3} and 2.6×10^9 cm^{-3} for peaks A, B and C, respectively, and presented in Table I.

4. Conclusion

Thermally stimulated current experiments in the high temperature range 100–300 K showed that there were three trapping centers at 400, 570 and 650 meV in $TlInS_2$ crystals. As the crystals studied are not intentionally doped, the observed levels are thought to originate from defects, created during the growth of crystals and/or unintentional impurities. Various methods are used to calculate the trap parameters and they agree well with each other. The retrapping process is negligible for these levels, as confirmed by the good agreement between the experimental results and the theoretical predictions of the model that assumes slow retrapping. Capture cross-sections of these traps were calculated to be 6.3×10^{-16}, 2.7×10^{-12}, and 1.8×10^{-11} cm^2. Also the concentrations of the traps were estimated to be 4.1×10^9, 0.9×10^9, and 2.6×10^9 cm^{-3}. The experiments on thermally stimulated current showed also the presence of an exponential distribution of hole-trapping states in $TlInS_2$ crystal in the high temperature range. The variation of one order

of magnitude in the trap density for every 800 meV was obtained.

References

[1] K.A. Yee, A. Albright, *J. Am. Chem. Soc.* **113**, 6474 (1991) and references therein.

[2] K.R. Allakhverdiev, *Solid State Commun.* **111**, 253 (1999).

[3] T.D. Ibragimov, I.I. Aslanov, *Solid State Commun.* **123**, 339 (2002).

[4] H. Hahn, B. Wellmann, *Naturwissenschaften* **54**, 42 (1967).

[5] D. Muller, F.E. Poltmann, H. Hahn, *Z. Naturforsch. B* **29**, 117 (1974).

[6] K.J. Range, G. Engert, W. Muller, A. Weiss, *Z. Naturforsch. B* **29**, 181 (1974).

[7] N. Kalkan, D. Papadopoulos, A.N. Anagnostopoulos, J. Spyridelis, *Mater. Res. Bull.* **28**, 693 (1993).

[8] M.P. Hanias, A.N. Anagnostopoulos, K. Kambas, J. Spyridelis, *Physica B* **160**, 154 (1989).

[9] M.P. Hanias, A.N. Anagnostopoulos, K. Kambas, J. Spyridelis, *Mater. Res. Bull.* **27**, 25 (1992).

[10] A.F. Qasrawi, N.M. Gasanly, *Cryst. Res. Technol.* **39**, 439 (2004).

[11] J.A. Kalomiros, A.N. Anagnostopoulos, *Phys. Rev. B* **50**, 7488 (1994).

[12] K.R. Allakhverdiev, T.G. Mammadov, R.A. Suleymanov, N.Z. Gasanov, *J. Phys., Condens. Matter* **5**, 1291 (2003).

[13] T.D. Ibragimov, I.I. Aslanov, *Solid State Commun.* **123**, 339 (2002).

[14] Nevin Kalkan, M.P. Hanias, A.N. Anagnostopoulos, *Mater. Res. Bull.* **27**, 1329 (1992).

[15] G.D. Guseinov, E. Mooser, E.M. Kerimova, R.S. Gamidov, I.V. Alekseev, M.Z. Ismailov, *Phys. Status Solidi* **34**, 33 (1969).

[16] M.Ya. Bakirov, N.M. Zeinalov, S.G. Abdullayeva, V.A. Gajiyev, E.M. Gojayev, *Solid State Commun.* **44**, 205 (1982).

[17] A. Aydinli, N.M. Gasanly, I. Yilmaz, A. Serpenguzel, *Semicond. Sci. Technol.* **14**, 599 (1999).

[18] V.M. Skorikov, V.I. Chmyrev, V.V. Zuev, E.V. Larina, *Inorg. Mater.* **38**, 751 (2002).

[19] Y. Kamitani, S. Maeta, *Jpn. J. Appl. Phys.* **39**, 115 (2000).

[20] E. Borchi, M. Bruzzi, S. Pirollo, S. Sciortino, *J. Phys. D, Appl. Phys.* **3**, L93 (1998).

[21] R. Chen, Y. Kirsh, *Analysis of Thermally Stimulated Processes*, Pergamon Press, Oxford 1981.

[22] R. Bube, *Photoelectronic Properties of Semiconductors*, Cambridge University Press, Cambridge 1992.

[23] N.S. Yuksek, N.M. Gasanly, H. Ozkan, O. Karci, *Acta Phys. Pol. A* **106**, 95 (2004).

[24] S. Özdemir, R.A. Suleymanov, E. Civan, T. Firat, *Solid State Commun.* **98**, 385 (1996).

[25] M. Isik, K. Goksen, N.M. Gasanly, H. Ozkan, *J. Korean Phys. Soc.* **52**, 367 (2008).

[26] N.S. Yuksek, N.M. Gasanly, H. Ozkan, *Semicond. Sci. Technol.* **18**, 834 (2003).

[27] A. Serpi, *J. Phys. D, Appl. Phys.* **9**, 1881 (1976).

[28] A. Bosacchi, B. Bosacchi, S. Franchia, L. Hernandez, *Solid State Commun.* **13**, 1805 (1973).

[29] A. Anedda, M.B. Casu, A. Serpi, I.I. Burlakov, I.M. Tiginyanu, V.V. Ursaki, *J. Phys. Chem. Solids* **58**, 325 (1997).

[30] P.C. Ricci, A. Anedda, R. Corpino, I.M. Tiginyanu, V.V. Ursaki, *J. Phys. Chem. Solids* **64**, 1941 (2003).

[31] T. Pisarkiewicz, *Opto-Electron. Rev.* **12**, 33 (2004).